High quality three-dimensional aluminum microwave cavities

Applied Physics Letters

High quality three-dimensional aluminum microwave cavities

Cite as: Appl. Phys. Lett. **117**, 070601 (2020); https://doi.org/10.1063/5.0016463
Submitted: 04 June 2020 . Accepted: 28 July 2020 . Published Online: 17 August 2020

M. Kudra, J. Biznárová, A. Fadavi Roudsari, J. J. Burnett, D. Niepce, S. Gasparinetti, B. Wickman, and P. Delsing

Applied Physics Letters ARTICLE scitation.org/journal/apl

High quality three-dimensional aluminum microwave cavities

Cite as: Appl. Phys. Lett. **117**, 070601 (2020); doi: 10.1063/5.0016463
Submitted: 4 June 2020 · Accepted: 28 July 2020 ·
Published Online: 17 August 2020

View Online Export Citation CrossMark

M. Kudra,[1,a] J. Biznárová,[1] A. Fadavi Roudsari,[1] J. J. Burnett,[2] D. Niepce,[1] S. Gasparinetti,[1] B. Wickman,[3] and P. Delsing[1,b]

AFFILIATIONS

[1]Department of Microtechnology and Nanoscience, Chalmers University of Technology, 412 96 Gothenburg, Sweden
[2]National Physical Laboratory, Hampton Road, Teddington TW11 0LW, United Kingdom
[3]Department of Physics, Chalmers University of Technology, 412 96 Gothenburg, Sweden

[a]Author to whom correspondence should be addressed: kudra@chalmers.se
[b]Electronic mail: per.delsing@chalmers.se

ABSTRACT

We present a comprehensive study of internal quality factors in superconducting stub-geometry three-dimensional cavities made of aluminum. We use wet etching, annealing, and electrochemical polishing to improve the as machined quality factor. We find that the dominant loss channel is split between the two-level system loss and an unknown source with a 40:60 proportion. A total of 17 cavities of different purity, resonance frequency, and size were studied. Our treatment results in reproducible cavities, with 10 of them showing internal quality factors above 80×10^6 at a power corresponding to an average of a single photon in the cavity. The best cavity has an internal quality factor of 115×10^6 at a single photon level.

Quantum information with superconducting circuits is a leading platform for realizing a practical quantum computer. One promising approach is to encode the information in harmonic oscillators.[1–5] Among different types of harmonic oscillators, three-dimensional (3D) cavities have long lifetimes[2,3] and have been successfully integrated with qubits.[1,6–9] Out of different 3D cavity geometries, stub-geometry 3D cavities have been demonstrated to have millisecond lifetimes[1] at a single photon level with strong dispersive coupling to the qubit. The quality factor of the cavity is a product of its lifetime, τ, and its resonant frequency, f_r: $Q = 2\pi f_r \tau$. Although a recipe on how to make these cavities can be found in Reagor *et al.*,[1] there is no systematic study on how the different parameters and treatments influence the internal quality factor. Here, we examine how different grades of aluminum, cavity height, cavity frequency, and three different treatments influence the internal quality factor of the stub-geometry cavity. We find that by etching and annealing the cavities, their internal quality factor reproducibly exceeds 80×10^6.

A drawing of a 3D cavity and its simulated electric field are presented in Fig. 1(a). Compared to a previous work by Reagor *et al.*,[1] we make a slight change in the geometry: we add a half sphere on top of the post to reduce the amplitude of the electric field on the surface of the post, as shown in Fig. 1(a).

The electric and magnetic fields are concentrated around the top and the bottom of the post, respectively, and they decay exponentially toward the lid of the cavity. Here, we used the eigenvalue solver of COMSOL Multiphysics® to calculate the resonance frequency and participation ratios of different loss channels[2] (formulas given below) and to optimize the diameter of the post with respect to the diameter of the cavity so that the participation ratio of the electric field is minimal at the surfaces. The resonance frequency of the stub geometry cavity is approximately defined by the length of the post as a quarter-wave resonator.

We study the effects of the following treatments on the internal quality factor. The first treatment is etching twice in an aluminum etchant (Transene aluminum etch A) for 2 h at 50 °C to remove approximately 100 μm of aluminum.[1] The cavities are placed in the acid with the opening facing up to prevent bubbles that form on the surface of the aluminum getting trapped. After removing cavities from the acid bath, we rinse them in water and further clean them in acetone and then isopropyl alcohol (IPA). The second treatment is annealing,[11] which is performed for three hours in a nitrogen atmosphere at 500 °C. The warming up of the furnace is gradual, and the speed is limited by the furnace that was available. It takes 1.5 h. The

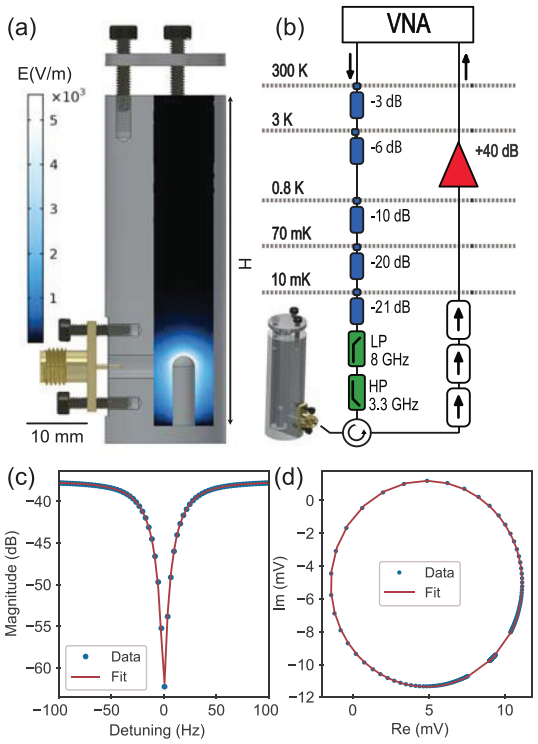

FIG. 1. (a) Drawing of the stub-geometry cavity with the simulated electric field amplitude displayed in the color scale. (b) Schematics of the experimental setup. Cavities are mounted at the mixing chamber of a dilution refrigerator (temperature T = 10 mK) and measured in reflection with a vector network analyzer (VNA). Example of the data fitted to a circle fit[10] (c) magnitude and (d) quadratures.

cooling down to room temperature takes approximately 4–5 h. The long cooling down time favors the relaxation of defects in the aluminum lattice and reduces the silicon content.[11] The third treatment is electrochemical polishing in a solution of phosphoric and sulfuric acids, with a ratio of 60:40. The results of a study on the roughness of aluminum samples[12] inspired us to electrochemically polish the cavities. The cavities are connected to the positive electrode of the voltage source, while a graphite rod is placed just above the central pin of the cavity as the cathode. We perform cycles of voltage sweeps from 0 to 15 V at a rate of 50 mV/s for about 1 h at 30 °C. Next, we increase the temperature to 60 °C and continue to sweep the voltage for another half an hour. This is followed by three cycles of sweeping the voltage at 50 mV/s until the current plateau that is characteristic for the diffusion-limited electropolishing regime[13] appears in the I–V curve (3–6 V depending on the cavity), whereupon the voltage is held constant at the plateau for 20 min. After electrochemical polishing, we rinse the cavities in water and clean them in acetone and then IPA in the same way as after etching.

After each treatment, we mounted the cavities to the mixing chamber of a dilution refrigerator inside a cryoperm shield, with no magnetic components inside the shield. We measured the cavities in reflection using cryogenic circulators and isolators, as shown in Fig. 1(b). We used the so-called circle fit[10] to simultaneously fit both quadratures in the in-phase and quadrature (IQ) plane,

$$S_{11} = ae^{i\alpha}e^{-i2\pi f\tau}\left(\frac{2Q_l/Q_c e^{i\phi}}{1+2iQ_l(f/f_r-1)}-1\right). \quad (1)$$

We fit the loaded (Q_l) and external (Q_c) quality factors, as well as the resonance frequency f_r. We then extract the internal quality factor ($1/Q_i = 1/Q_l - 1/Q_c$). We also fit the measurement setup parameters a, α, and τ, where a is the background offset accounting for the net attenuation of the signal sent from the vector network analyzer [Fig. 1(b)], α is a global phase offset, and τ is the electrical delay in our lines. An example of the fit is given in Figs. 1(c) and 1(d).

The results are summarized in Table I and Fig. 2. Each cavity is represented by a symbol and given a name (C_{1-17}). The material, height, and resonance frequency of each cavity are listed in the table. The internal quality factor of the cavities at a single photon level is shown in Figs. 2 and 3, where each treatment is represented by a color. For the results presented in Figs. 2(a)–2(c), the order of the colored bars from left to right is based on the treatment sequence that the as-machined cavity has received. The cavities may have undergone some, or all of the treatments. Cavities C_{15-17} [Fig. 2(c)] were machined out of an aluminum alloy 6081, which contains between 96% and 98% aluminum and the rest is mostly magnesium, silicon, and manganese. Regardless of the treatment, the internal quality factor of these cavities did not improve significantly, and the best quality factor was about 12 × 10^6. We thus conclude that quality factors of cavities C_{15-17} are limited by the impurities in the material.

Cavities made from 5N (99.999%) aluminum (C_{1-10}; Figs. 2 and 3 and Table I) are measured as-machined, after etching, and then the etched cavities were annealed [Fig. 3(a)]. After machining, there is widespread quality factors from 8 × 10^6 all the way to 82 × 10^6, with

TABLE I. Measured single photon internal quality factors of 17 aluminum cavities, either after etching and annealing (cavities C_{1-14} and C_{16}) or after etching (cavities C_{15} and C_{17}).

Symbol	Cavity	Material	Height (mm)	f_r (GHz)	Q_i (10^6)	τ_{int} (ms)
●	C_1	5N	35	7.431	83	1.79
⬢	C_2	5N	40	7.417	66	1.43
✖	C_3	5N	45	7.425	81	1.75
▼	C_4	5N	50	7.417	93	2.02
▲	C_5	5N	50	7.427	79	1.71
◀	C_6	5N	50	7.428	91	1.96
▶	C_7	5N	50	7.427	82	1.77
■	C_8	5N	50	6.476	86	2.11
⬟	C_9	5N	50	5.478	94	2.74
◆	C_{10}	5N	50	4.501	115	4.09
✚	C_{11}	4N	35	5.932	30	0.81
⧫	C_{12}	4N	50	7.437	101	2.16
⬢	C_{13}	4N	50	5.928	75	2.03
★	C_{14}	4N	50	5.923	84	2.27
…	C_{15}	6081	35	5.976	5	0.13
…	C_{16}	6081	50	5.929	12	0.34
…	C_{17}	6081	50	5.939	7	0.21

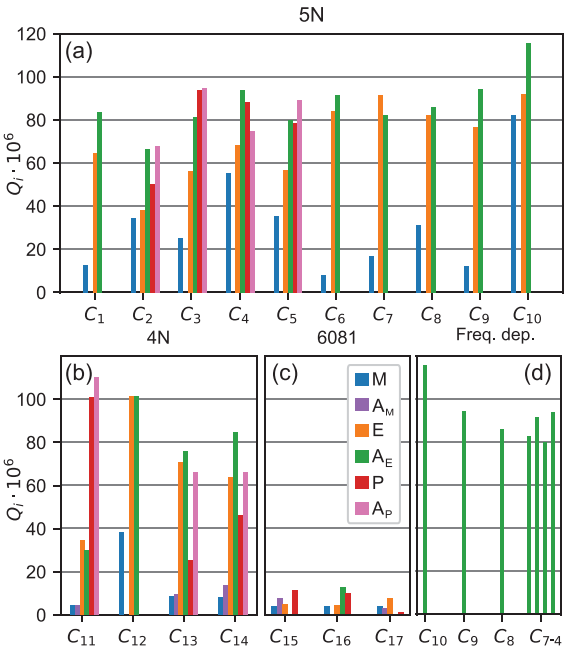

FIG. 2. Single photon internal quality factor Q_i of the cavities after each treatment, for cavities made out of (a) 5N, (b) 4N, and (c) 6081 aluminum. M-after machining; A_M-after annealing (applied to cavities C_{11}, C_{13-15}, and C_{17}); E-after etching; A_E-after etching and annealing; P-after etching, annealing, and electrochemical polishing; and A_P-after etching, annealing, and electrochemical polishing, and a second annealing step. (d) Dependence of the single photon internal quality factor on resonance frequency after etching and annealing. Cavities C_{10-4} are made from 5N aluminum with resonance frequencies ranging from 4.5 GHz (C_{10}) to 7.5 GHz (C_{7-4}). See Table I for exact frequencies.

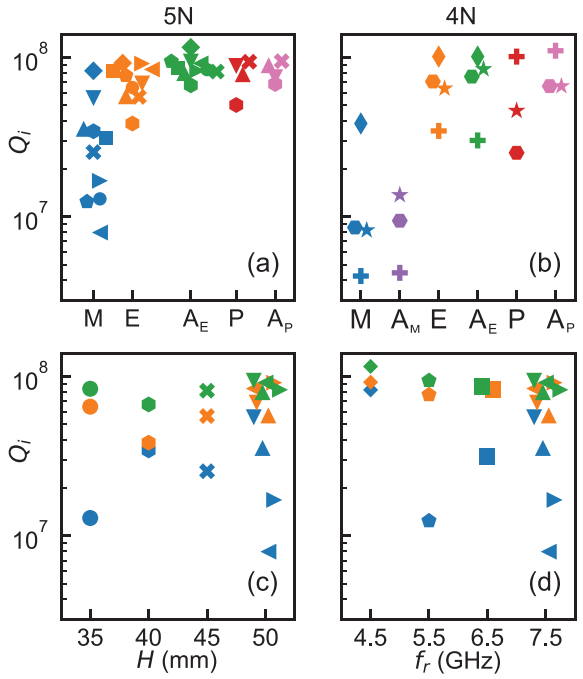

FIG. 3. (a) and (b) Single photon internal quality factor as a function of the treatment applied for the cavities made from (a) 5N (99.999%) and (b) 4N (99.99%) aluminum. Dependence of the internal quality factor on the (c) height of the cavity (cavities C_{1-7}) and (d) resonance frequency (cavities C_{4-10}). Individual cavities are coded with symbols listed in Table I, and treatments are coded with same colors as in Fig. 2. The treatments were sequentially applied in the order presented in (a) for 5N cavities and (b) for 4N cavities.

an average quality factor of 31×10^6. We attribute this to defects caused by machining and possible impurities that can be introduced.

After etching, the quality factor increased for all of the cavities, leading to an average quality factor of 71×10^6 with a spread of 54×10^6 between the maximum and minimum quality factors. Etching around 100 μm of aluminum of the cavity surface seems to remove most of the machining defects. However, after etching, aluminum oxide forms on the surface in a cleanroom ambient atmosphere in an uncontrolled manner; therefore, it can cause some spread in the results. During the annealing process, the increased mobility of the atoms allows for restoring the defects in the aluminum lattice and the oxide and the interface of the two. The average quality factor after annealing is 88×10^6, and the spread in the quality factor is reduced to 49×10^6. Cavities C_{4-7} are nominally identical. The internal quality factors of these four cavities are within 8% of their average value (Table I).

In Figs. 3(a) and 3(b), we compare the performance of the cavities made from 5N (99.999%) aluminum (C_{1-10}) and 4N (99.99%) aluminum (C_{11-14}). While it is not possible to predict which as-machined cavity will have a better quality factor after the treatments, both types show an average quality factor of above 80×10^6 after etching and annealing (green). Using the higher purity (5N) aluminum would not give us any leverage unless the more dominant sources of loss (discussed later) are eliminated.

A total of seven cavities made from 5N (C_{2-5}) and 4N (C_{11} and C_{13-14}) aluminum were electrochemically polished [see Figs. 2, 3(a), and 3(b) in red]. Although the surface of all the cavities got a mirror like finish after the polishing step, the improvement of the internal quality factor was not conclusive. For example, cavity C_{11} had a Q_i of 30×10^6 after etching and annealing and the quality factor improved to 100×10^6 after adding the polishing step. However, compared to the etched and annealed Q_i, polishing the other cavities either deteriorated the Q_i or just slightly improved it [see Figs. 2, 3(a), and 3(b) in red). Adding an annealing step after the polishing step [see Figs. 2, 3(a), and 3(b) in pink] improved the polished Q_i slightly. More investigations are needed to make electrochemical polishing a more reliable procedure for improving the internal quality factor.

With the above observations, we set out to determine the dominant loss mechanism. To explore the influence of seam loss, we made cavities C_{1-7} of varying heights [35–50 mm; see Fig. 1(a)]. The participation of the seam loss exponentially decays with the height of the cylindrical waveguide section,[1] so we would expect to see this trend if seam loss was the limiting loss factor. No such trend is visible [Fig. 3(c)]. After etching and annealing, regardless of the height, all of the cavities show similar Q_i. Therefore, we conclude that seam loss is not the limiting factor for cavities longer than 35 mm at this quality factor level.

Next, we investigate the influence of resonance frequency on the internal quality factor. The resonance frequency of the cavities C_{4-10} ranges from 4.5 to 7.5 GHz. Here, the length of the center pin was

changed to get the desired resonance frequency. The length of the waveguide was simultaneously adjusted so that the seam loss has the same participation ratio for all of them. For the cavities to meet these two criteria, the total height of the cavity from the bottom of the pin to the lid should be kept fixed [H in Fig. 1(a)]. There is a slight trend of lower frequencies having higher internal quality factor [Figs. 3, 2(d), and Table I]. This could be attributed to the lower density of states of the two-level systems (TLSs) at lower frequencies.[14]

The dependence of Q_i on power and temperature for cavity C_{10} after etching and annealing is presented in Fig. 4. We fitted the internal quality factor (Q_i) as a function of the average number of photons to a standard TLS model[16–19] [Fig. 4(a)],

$$1/Q_i = F\delta_{TLS}\tanh\left(\frac{hf_r}{2kT}\right)(1+n/n_c)^{-\beta} + \frac{1}{Q_{res}}. \quad (2)$$

The average number of photons n is estimated using the formula $n = 4Q_l^2P/(Q_c\hbar(2\pi f_r)^2)$, where the power sent to the cavity P is estimated from the value at the source and the known line attenuation. The first parameter we extract from the fit is the product of the participation ratio of the electric field (F) and the two level system loss tangent (δ_{TLS}). We simulated the participation ratio of the electric field $F = t_{ox}\int\int|E|^2dS/\epsilon_r\int\int\int|E|^2dV = 3.6\times10^{-7}$, assuming the thickness of the oxide layer $t_{ox} = 5$ nm and the relative permittivity of aluminum oxide $\epsilon_r = 10$. This yields the loss tangent of the surface oxide of $\delta_{TLS} = 9.8\times10^{-3}$. In the planar circuits, the participation ratio of TLSs is on the order of $(10^{-3}-10^{-4})$,[20,21] three to four orders of magnitude more than our simulated participation ratio F. This can explain the higher Q factor compared to the planar circuits. The second fit parameter is the critical photon number $n_c = 1.3\times10^6$. N_c is the number of photons that produce an electric field strength that starts to saturate a sizeable fraction of the TLSs. In contrast to planar circuits where the critical photon number is close to unity,[4,5,22] our 3D cavities show six orders of magnitude higher critical photon number. From the simulation, we can extract the strength of the electric field $E_c = 2.9$ V/m at the top of the post that corresponds to the critical photon number. The critical electric field strength E_c compares well with the critical fields found in on-chip parallel plate capacitors [$E_c = (0.5–15)$ V/m].[23] The third fitting parameter is $\beta = 0.11$, which is usually found to be around 0.2 in both planar[24,25] and 3D resonators.[3] Finally, the quality factor of the residual loss mechanism, $Q_{res} = 193\times10^6$, is the last fitting parameter. Given the difference between the high power (Q_{res}) and the low power internal quality factors, we calculate that the TLSs contribute to $1-Q_{low}/Q_{res} = 40\%$ of the total loss in the resonator at low power. We are not able to present data for higher photon numbers since the resonator becomes non-linear; the resonance frequency shifts to lower frequencies, and the line shape is no longer reliably fitted by the circle fit routine. At low photon numbers, the last two data points seemingly deviate from the model. We ascribe this deviation to the statistical uncertainty. The latter is underrepresented by the error bars shown in the plot, which reflects the confidence interval associated with the fit parameters. Considering the power dependence of other cavities in the same power range (not shown), we observe no evidence for a systematic behavior. The other cavities show a similar dependence of internal quality factor to power.

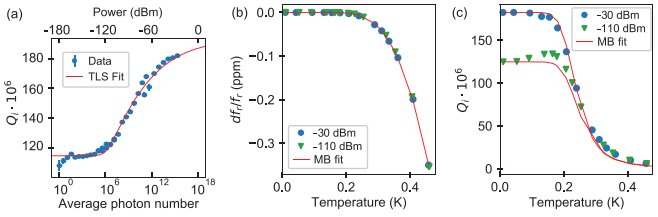

FIG. 4. (a) Internal quality factor as a function of the average number of photons in the C_{10} cavity (after etching and annealing) fitted to the TLS model [Eq. (2)]. The top axis shows the estimated power sent to the cavity. (b) and (c) The temperature dependence of (b) frequency and (c) internal quality factor for two different input powers (symbols) and the Mattis–Bardeen fit[15] (solid lines). Frequency and internal quality factor are simultaneously fitted using two fitting parameters: critical temperature T_c and kinetic inductance ratio α.

By sweeping the temperature, we can probe the sensitivity of the cavity to thermally excited quasiparticles. In Figs. 4(b) and 4(c), we show a Mattis–Bardeen fit[15] of the frequency and the internal quality factor as a function of temperature. The fit is in the clean limit for a bulk superconductor,[15] and it has two fitting parameters. The first one is the bulk aluminum critical temperature $T_c = 1.18$ K, which is quite close to the literature value.[26] The second one is the kinetic inductance ratio $\alpha = 5.07\times10^{-5}$. α is given by $\lambda\cdot p_H$, where $p_H = \int\int|H|^2dS/\int\int\int|H|^2dV$ is simulated to be $p_H = 814.8$ m^{-1}. Thus, we can extract the effective penetration depth $\lambda = 62$ nm, which compares relatively well to the textbook values.[15] Both frequency dependence and the internal quality factor dependence were simultaneously fitted with the same critical temperature and kinetic inductance. The slight increase in the internal quality factor between 10 mK and 200 mK for the low power trace [the green triangles in Fig. 4(c)] is due to the tanh dependence of the TLS given by Eq. (2).[3] If we assume that the Q-value at high power, Q_{res}, was caused by quasiparticles, the equivalent temperature of the quasiparticles would be 223 mK. We find it unlikely that the cavity is that hot or that the non-equilibrium density of the quasiparticles is that high, and we therefore suppose that Q_{res} is due to some other unknown loss.

In conclusion, we have demonstrated that etching and annealing 3D cavities result in a reproducible recipe to make aluminum cavities with internal quality factors at a single photon level exceeding 80×10^6. Electrochemical polishing improved the quality factors of some cavities but reduced the quality factors of others. More research is needed to make this process more reproducible. Once the total height of the cavity exceeds 35 mm, seam loss is not a limiting factor. TLS loss contributes to around 40% of the total loss at low power. The difference between 4N and 5N cavities is not visible at internal quality factors around 100×10^6.

The authors thank Mats Myremark and Lars Jönsson for machining the cavities. This work was supported by the Knut and Alice Wallenberg Foundation via the Wallenberg Center for Quantum Technology (WACQT) and by the Swedish Research Council. The authors acknowledge the use of Chalmers Myfab for the treatment of the cavities. J.J.B. acknowledges financial support from the Industrial Strategy Challenge Fund Metrology Fellowship as part of the UK government's Department for Business, Energy and Industrial Strategy.

DATA AVAILABILITY

The data that support the findings of this study are available from the corresponding author upon reasonable request.

REFERENCES

[1]M. Reagor, W. Pfaff, C. Axline, R. W. Heeres, N. Ofek, K. Sliwa, E. Holland, C. Wang, J. Blumoff, and K. Chou, Phys. Rev. B **94**, 014506 (2016).
[2]M. Reagor, H. Paik, G. Catelani, L. Sun, C. Axline, E. Holland, I. M. Pop, N. A. Masluk, T. Brecht, and L. Frunzio, Appl. Phys. Lett. **102**, 192604 (2013).
[3]A. Romanenko and D. Schuster, Phys. Rev. Lett. **119**, 264801 (2017).
[4]D. Zoepfl, P. R. Muppalla, C. M. F. Schneider, S. Kasemann, S. Partel, and G. Kirchmair, AIP Adv. **7**, 085118 (2017).
[5]J. Burnett, A. Bengtsson, D. Niepce, and J. Bylander, J. Phys.: Conf. Ser. **969**, 012131 (2018).
[6]B. Vlastakis, G. Kirchmair, Z. Leghtas, S. E. Nigg, L. Frunzio, S. M. Girvin, M. Mirrahimi, M. H. Devoret, and R. J. Schoelkopf, Science **342**, 607–610 (2013).
[7]N. Ofek, A. Petrenko, R. Heeres, P. Reinhold, Z. Leghtas, B. Vlastakis, Y. Liu, L. Frunzio, S. M. Girvin, and L. Jiang, Nature **536**, 441–445 (2016).
[8]L. Hu, Y. Ma, W. Cai, X. Mu, Y. Xu, W. Wang, Y. Wu, H. Wang, Y. Song, C.-L. Zou *et al.*, Nat. Phys. **15**, 503 (2019).
[9]E. Flurin, N. Roch, J. D. Pillet, F. Mallet, and B. Huard, Phys. Rev. Lett. **114**, 090503 (2015).
[10]S. Probst, F. B. Song, P. A. Bushev, A. V. Ustinov, and M. Weides, Rev. Sci. Instrum. **86**, 024706 (2015).
[11]D. L. Creedon, M. Goryachev, N. Kostylev, T. B. Sercombe, and M. E. Tobar, Appl. Phys. Lett. **109**, 032601 (2016).
[12]J. Biznárová, "Electropolishing of superconducting cavities for quantum memory applications," Master's thesis (Chalmers University of Technology, 2019).
[13]D. Landolt, Electrochim. Acta **32**, 1 (1987).
[14]S. T. Skacel, C. Kaiser, S. Wuensch, H. Rotzinger, A. Lukashenko, M. Jerger, G. Weiss, M. Siegel, and A. V. Ustinov, Appl. Phys. Lett. **106**, 022603 (2015).
[15]J. Gao, "The physics of superconducting microwave resonators," Ph.D. thesis (California Institute of Technology, 2008).
[16]J. J. Burnett, A. Bengtsson, M. Scigliuzzo, D. Niepce, M. Kudra, P. Delsing, and J. Bylander, npj Quantum Inf. **5**, 54 (2019).
[17]P. V. Klimov, J. Kelly, Z. Chen, M. Neeley, A. Megrant, B. Burkett, R. Barends, K. Arya, B. Chiaro, Y. Chen, A. Dunsworth, A. Fowler, B. Foxen, C. Gidney, M. Giustina, R. Graff, T. Huang, E. Jeffrey, E. Lucero, J. Y. Mutus, O. Naaman, C. Neill, C. Quintana, P. Roushan, D. Sank, A. Vainsencher, J. Wenner, T. C. White, S. Boixo, R. Babbush, V. N. Smelyanskiy, H. Neven, and J. M. Martinis, Phys. Rev. Lett. **121**, 090502 (2018).
[18]S. Schlör, J. Lisenfeld, C. Müller, A. Bilmes, A. Schneider, D. P. Pappas, A. V. Ustinov, and M. Weides, Phys. Rev. Lett. **123**, 190502 (2019).
[19]J. M. Martinis, K. B. Cooper, R. McDermott, M. Steffen, M. Ansmann, K. D. Osborn, K. Cicak, S. Oh, D. P. Pappas, R. W. Simmonds, and C. C. Yu, Phys. Rev. Lett. **95**, 210503 (2005).
[20]C. E. Murray, IEEE Trans. Microwave Theory Tech. **68**, 3263–3270 (2020).
[21]C. Wang, C. Axline, Y. Y. Gao, T. Brecht, Y. Chu, L. Frunzio, M. Devoret, and R. J. Schoelkopf, Appl. Phys. Lett. **107**, 162601 (2015).
[22]G. Calusine, A. Melville, W. Woods, R. Das, C. Stull, V. Bolkhovsky, D. Braje, D. Hover, D. K. Kim, X. Miloshi *et al.*, Appl. Phys. Lett. **112**, 062601 (2018).
[23]H. Paik and K. D. Osborn, Appl. Phys. Lett. **96**, 072505 (2010).
[24]P. Macha, S. van Der Ploeg, G. Oelsner, E. Il'ichev, H.-G. Meyer, S. Wünsch, and M. Siegel, Appl. Phys. Lett. **96**, 062503 (2010).
[25]J. Burnett, J. Sagar, O. W. Kennedy, P. A. Warburton, and J. C. Fenton, Phys. Rev. Appl. **8**, 014039 (2017).
[26]R. Pöpel, *Superconducting Quantum Electronics* (Springer, 1989), pp. 44–78.